Relaxation dynamics of labyrinthine submonolayer films

Koichi Sudoh*, Masakazu Okano, Toshiharu Irisawa[a],
Kiiko Katsuno (Matsumoto)[b], and Makio Uwaha[c]
The Institute of Scientific and Industrial Research,
Osaka University, 8-1 Mihogaoka, Ibaraki, Osaka 567-0047, Japan
[a]*Computer Center, Gakushuin University,*
1-5-1 Mejiro, Toshima-ku, Tokyo 171-8588, Japan
[b]*Seikei University, 3-3-1, Kichijoji-Kitamachi,*
Musashino-shi, Tokyo, 180-8633 Japan
[c]*Department of Physics, Nagoya University,*
Furo-cho, Chikusa-ku, Nagoya 464-8602, Japan

(Dated: October 1, 2012)

Abstract

To explore the relaxation process of percolating labyrinthine submonolayer films, we observe in real-time the evolution of a submonolayer film with a coverage of ~ 0.7 monolayer on $SrTiO_3(001)$ at 670 °C using scanning tunneling microscopy. We find that the characteristic length begins to increase after an incubation time. During the incubation time, percolating grooves are segmented by local pinch-off events predominantly driven by thermal fluctuations. The occurrence frequency of the pinch-off events markedly decreases with an increase in the characteristic length. In the second stage, reshaping of the disconnected irregular vacancy islands occurs by edge diffusion. Finally, small vacancy islands disappear via Ostwald ripening by terrace diffusion.

* Corresponding author.Tel:+81-6-6879-8401; Fax:+81-6-6879-8404;
E-mail address: sudoh@sanken.osaka-u.ac.jp

Progress of nanodevice technology relies on fine control of surface morphology. Understanding of the evolution of nanoscale surface features is crucial to achieve such surface control. Atomically controlled growth processes, such as molecular beam epitaxy and pulsed laser deposition, involve evolution of the surface composed of two atomic layers separated by monolayer steps. Relaxation of such quasi two-dimensional (2D) morphologies by surface diffusion has been an issue of extensive study for technologically important materials such as $SrTiO_3$ [1–5]. In addition, there is fundamental interest in the relaxation processes on the surface since they are typical systems that exhibit coarsening dynamics in phase separation phenomena.

The morphological features of submonolayer films markedly change depending on their coverage [6]. For sufficiently low and high coverages, isolated clusters of adatoms and vacancies are formed, respectively. It is well known that such systems generally relax through Ostwald ripening process by terrace diffusion. The kinetics of Ostwald ripening has been extensively studied and rigorous models are available to reproduce the observed coarsening process [7, 8]. On the other hand, for intermediate coverages (namely around 0.5 monolayer), the film morphology becomes labyrinthine because the adatom clusters percolate through the surface. The relaxation of such films is analogous to the phase separation in 2D through spinodal decomposition [9]. The essential difference in the relaxation of such labyrinthine morphologies from that of isolated clusters is that the diffusion along the film edge and the diffusion across the terraces conspire to induce morphological changes [10]. The competition between the edge diffusion and the terrace diffusion leads to possibilities of diverse relaxation pathways depending on microscopic details of the system. Although many efforts have been devoted to address this issue [11, 12], our understanding of the relaxation dynamics of films at intermediate coverages is still very poor.

In this letter we study the relaxation dynamics of percolating labyrinthine films at an intermediate coverage, performing real time scanning tunneling microscope (STM) observations of a homoepitaxial film on a $SrTiO_3(001)$ surface. We reveal time evolution from a labyrinthine morphology with a characteristic length of a few nanometers to a droplet pattern of a few tens of nanometers. The growth of the characteristic length involves an incubation period, during which the percolating vacancy islands are segmented through local pinch-off events by thermal fluctuations. Then coarsening of the disconnected islands proceeds through reshaping by edge diffusion and finally through Ostwald ripening by terrace

diffusion.

The experiments were performed in a ultrahigh vacuum chamber with a base pressure of 1.0×10^{-8} Pa. Samples were cut from a Nb doped $SrTiO_3(001)$ single crystal. An atomically flat (001) surface was prepared by annealing the sample at around 800 °C. Both deposition of $SrTiO_3$ and STM observation of morhological relaxation were performed at 670 °C. In this study, we apply an STM nanofabrication technique to prepare an incomplete homoepitaxial film. First, a positive bias voltage in the range of 5–10 V is applied to the sample at the elevated temperature while the STM feadback loop is on. This makes the STM tip be contaminated with $SrTiO_3$ because an atomic transport from the sample surface to the STM tip is induced. Then the contaminated STM tip is randomly moved in an atomically flat surface region of a few hundred nanometers squared, while applying a negative bias voltage, 5–10 V, to the sample and the STM feadback loop is on. This causes random deposition of $SrTiO_3$ on the sample surface in the neighborhood of the STM tip. Within the deposited region we can find an area where a homogeneous submonolayer film is formed locally. STM data acquisition was typically initiated within a few minutes after preparation of the submonolayer film. Without changing the substrate temperature, the morphological change was monitored by STM at a rate of 10–30 s/frame.

Figure 1 shows the morphological evolution of a submonolayer film with a coverage of ∼70 % during annealing at 670 °C. The initial surface shows a labyrinthine film morphology where narrow vacancy grooves percolate through the imaged region [Fig. 1(a)]. This labyrinthine feature resembles films with intermediate coverages formed by molecular beam epitaxy on metal surfaces [13]. We find that the initially percolating vacancy pattern evolves into an ensemble of 2D vacancy islands. During the evolution the film coverage does not change significantly, implying that the relaxation advances by surface mass transport without sublimation.

To quantify the observed morphological evolution, we measure the characteristic length from the STM images. According to a previous study[10], we define the characteristic length L as the position of the first zero of the height correlation function,

$$G(\boldsymbol{r}) = \langle h(\boldsymbol{0})h(\boldsymbol{r})\rangle - \langle h\rangle^2 \tag{1}$$

where $h(\boldsymbol{r})$ is the discrete surface height at the position $\boldsymbol{r}$. Figure 1(e) shows a log-log plot of the obtained time dependence of the characteristic length. The plot does not show a

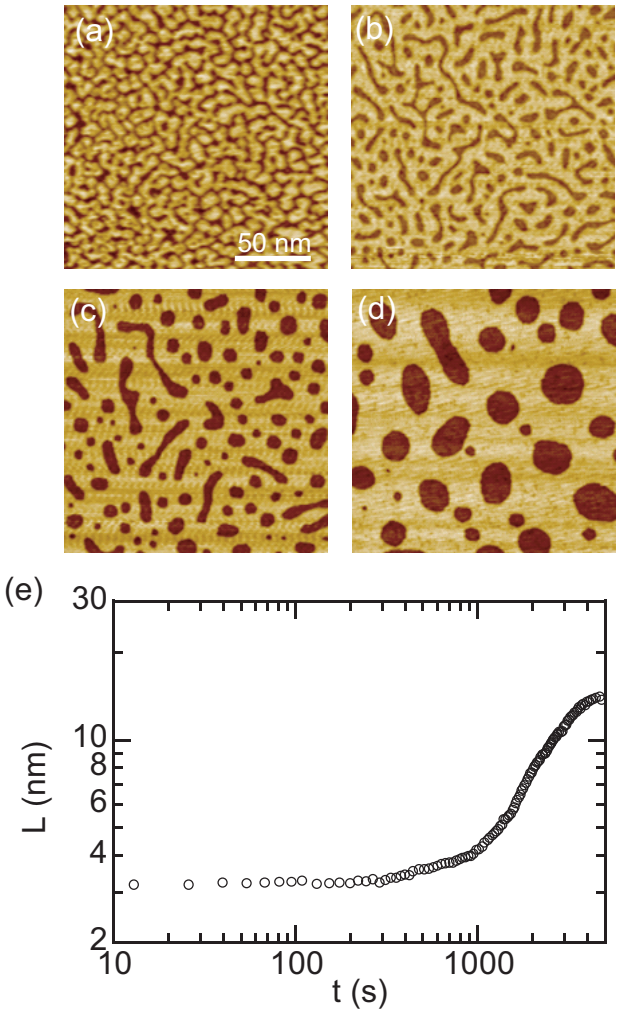

FIG. 1. Sequence of STM images showing the morphological relaxation of a labyrinthine homoepitaxial film on a $SrTiO_3(001)$ surface at 670 °C. The images (a)-(d) show the morphologies at times 0 s, 993 s, 1727 s, and 4735 s, respectively. (e)A logarithmic plot of the characteristic length L as a function of time.

single power law dependence, since the morphology does not evolve in a self-similar fashion, as observed in the images.

A distinct feature of Fig. 1(e) is that the characteristic length remains constant until $\sim$ 300 s. STM images in Figs. 2(a), (b) and (c) reveal the morphological change that has occurred during this incubation period. The percolating narrow vacancy grooves are broken up by local pinch-off events as indicated by arrows in the STM images. The effect of a pinch-off event on the film morphology is confined to the immediate vicinity of the pinch-off site, so that the widths of the grooves and the monolayer films do not change appreciably. Thus

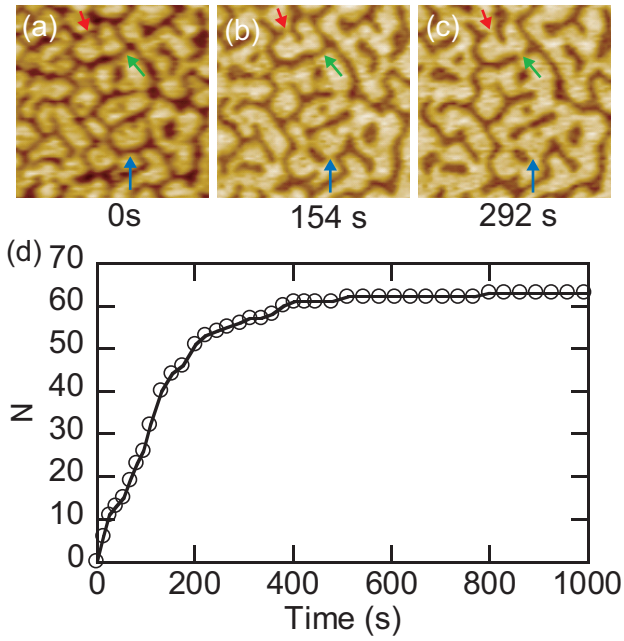

FIG. 2. The STM images (60 nm × 60 nm) of (a), (b) and (c) show the morphologies at 0s, 154s and 292s, respectively. The sites where a pinch-off event occurs are indicated by arrows. (d)The accumulated occurrence number N of pinch-off events is plotted as a function of time.

the characteristic length does not increase during this period. In Fig. 2(d), accumulated numbers of the pinch-off events in the observed area are plotted as a function of time. The occurrence is limited to the incubation period and suppressed as the characteristic length increases.

The sequence of STM images in Fig. 3 shows the evolution of the disconnected vacancy islands produced by the pinch-off events after the incubation period. Since the number N of pinch-off events is not very large, large and irregular-shaped vacancy islands are formed via random pinch-off of the percolated vacancy during the incubation period. We can see reshaping of the irregular-shaped vacancy islands and Ostwald ripening process in these later stages. Figure 3(e) shows the time evolution of the area of the individual vacancy islands indicated in the STM images. The area of each vacancy island does not change significantly until $\sim$ 1400 s. Thus, we consider that only shape change occurs by edge diffusion during this period, although we cannot exclude some contribution from terrace diffusion in the groove. This result is consistent with the previous observation of wormlike islands on metal surfaces [13]. In the later stages, Ostwald ripening occurs, i.e., large vacancy islands grow while small ones shrink and disappear by terrace diffusion between islands. This transition

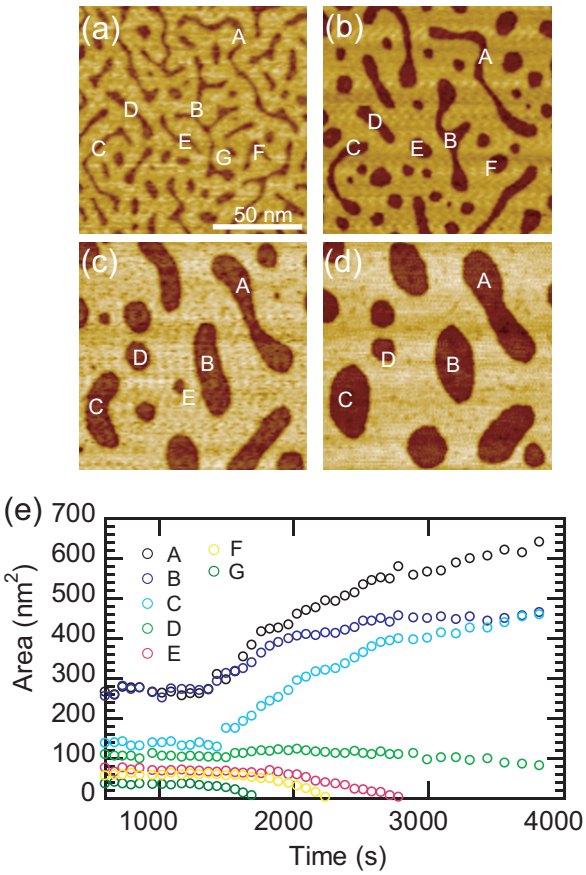

FIG. 3. (a)-(d)STM images showing the morphological evolution of disconnected irregular-shaped vacancy islands. The images (a)-(d) show the morphologies at 608 s, 1534 s, 2516 s, and 3925 s, respectively. (e)The time variation of the areas of the vacancy islands A-G indicated in the STM images.

of the dominant mass transport mechanism is reasonable because the driving force for edge diffusion becomes weak when the shape of a vacancy island approaches to the equilibrium one.

Our observation shows that a pinch-off event enables a more efficient morphological relaxation than retaining the percolated feature. When a narrow vacancy groove is disconnected by a pinch-off event, a pair of steps with very large curvatures is created at the cut ends. The newly formed steps are highly mobile because of their reduced Gibbs-Thomson chemical potential, and the cut ends quickly retreat from each other. We consider that the pinch-off events occur predominantly by an incidental collision of the steps due to fluctuations, because its occurrence is limited to the early stages where the characteristic length is small as

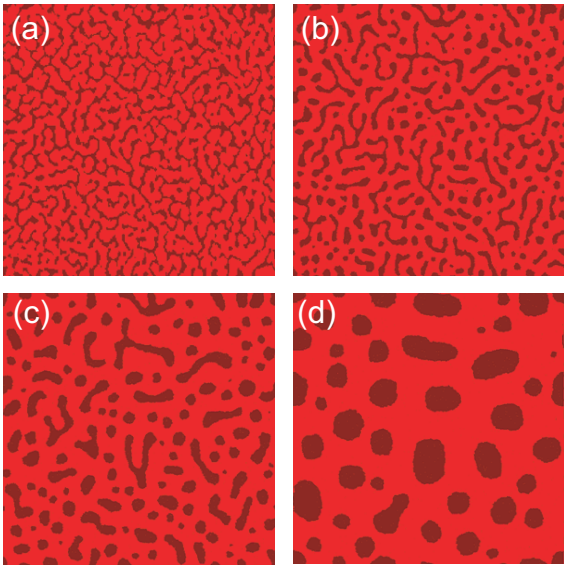

FIG. 4. Evolution of a labyrinthine film obtained by a kinetic MC simulation.

shown in Fig. 2. Previously, Erlebacher and Aziz [14] invoked the pinch-off process driven by the step fluctuations to understand the relaxation kinetics of a rippled surface by terrace diffusion. According to their result on the kinetics of pinch-off in the diffusion limited case, the average waiting time before pinch-off occurs for a pair of parallel steps increases very rapidly with increase in the separation between the steps. This strongly suggests that the occurrence of pinch-off events become suppressed markedly with an increase in the characteristic length, as observed in our experiment, although the rate limiting process for the step fluctuation in the experiment is still unclear. It has been reported that pinch-off occurs during deterministic evolution of wormlike vacancy islands by edge diffusion on metal surfaces [13]. However, we consider that the deterministic evolution is not dominant in our pinch-off events because some of them (indicated by red and blue arrows in Fig. 2) occur at apparently concave part of a groove. Although the elastic step-step interaction may play a role in the pinch-off events, we could not specify its effect at present.

To understand the observed relaxation process involving an incubation time in more detail, we performed kinetic Monte Carlo simulations employing a simple solid on solid model [3, 15]. We simulate the relaxation starting from the structure shown in Fig. 1(a). The original STM image of 200 nm $\times$ 200 nm has 256 pixels $\times$ 256 pixels. After binarizing the image the 256 $\times$ 256 image on the square lattice was expanded to 1024 $\times$ 1024 and used as the intial pattern of the simulation with an artifical periodic boudary condition.

The lattice constant in the simulation corresponds to 0.19 nm, which is roughly half of the lattice constant of $SrTiO_3$. The time evolution of the simulation is given by repetition of the following procedure: 1) choose a movable atom i (atoms surrounded by four nearest neighbors are immobile), 2) choose one of its four neigboring sites f for the destination, 3) calculate the initial energy E_i and the final energy E_f, 4) the move i to f is accepted with the probability $\theta(E_i - E_f) + \theta(E_f - E_i)e^{(E_i - E_f)/k_{\rm B}T}$, where $\theta(x)$ is the step function. The model includes the nearest neighbor and the second neighbor lateral bond energies: $-E_1/k_{\rm B}T = -2.0$ and $-E_2/k_{\rm B}T = -0.96$. Figure 4 shows a typical pattern evolution obtained in the simulation. The snapshots, (a), (b), (c) and (d) show the patterns at simulation times of 0, 2.86×10^5, 2.00×10^6 and 2.23×10^7, respectively[16]. They are chosen as to make the respective characteristic lengths comparable with those of Figs. 1(b), (c) and (d). With a proper choice of the energy parameters, characteristic feature of the relaxation, i.e., pinch-off of narrow grooves, reshaping of elongated vacancy islands and disappearance of small vacancy islands, are reproduced. The simulation also reproduces the existence of an incubation time for the growth of the characteristic length. We note that we could not obtain a linear relationship of time scale between the experiment and the simulation, although we have tried many other sizes and parameters, including the Schowoebel barrier etc. Discussion about this discrepancy of the time scale and the detailed analysis of our MC simulation results will be reported elsewhere.

The real microscopic processes involved in the surface relaxation of multicomponent crystals with a complicated unit cell such as $SrTiO_3$ must be more complicated than those assumed in the simulation model[17]. In this work we could not derive information on the form of species responsible for the surface diffusion from our STM observations. We believe that diffusion of adsorbed particles, namely atoms or atomic clusters, rather than vacancies is dominant, because the activation energy for creation of an adatom at a kink site is much smaller than that for excitaion of an adatom-vacancy pair on a terrace site.

In summary, we have observed in real time, how percolating labyrinthine grooves in a submonolayer film evolve into disconnected vacancy islands. The characteristic length begins to increase after an incubation period, during which the percolating grooves are disconnected through pinch-off events induced by fluctuations. In the second stage, the morphology evolves via reshaping of irregular shaped vacancy islands by edge diffusion without pinch-off. Finally, Ostwald ripening of the vacancy islands proceeds by terrace diffusion. Since the

simple simulation model reproduces the observed pattern evolution, our scheme is not specific to $SrTiO_3$ but a more general scenario for the surface relaxation phenomena. Detailed analysis and comparison with the simulation will be published elsewhere.

ACKNOWLEDGMENTS

The work was supported by Grants-in-Aid from the Japan Society for the Promotion of Science.

---

[1] M. Lippmaa, M. Kawasaki, A. Ohtomo, T. Sato, M. Iwatsuki, H. Koinuma, Appl. Surf. Sci. **130-132** (1998) 582.

[2] A. Fleet, D. Dale, A. R. Woll, Y. Suzuki, and J. D. Brock, Phys. Rev. Lett. **96** (2006) 05508.

[3] T. Irisawa, K. Matsumoto, K. Sudoh, H. Iwasaki, and M. Uwaha, Surf. Sci. **602** (2008) 2880.

[4] J. Chang, Y. Park, J. Lee, and S. Kim, J. Cryst. Growth **311** (2009) 3771.

[5] J. D. Ferguson, G. Arikan, D. S. Dale, A. R. Woll, and J. D. Brock, Phys. Rev. Lett. **103** (2009) 256103.

[6] J. -M. Wen, J. W. Evans, M. C. Bartelt, J. W. Burnett, and P. A. Thiel, Phys. Rev. Lett. **76** (1996) 652.

[7] N. C. Bartelt, W. Theis, and R. M. Tromp, Phys. Rev. B **54** (1996) 11741.

[8] S. Nie, N. C. Bartelt, and K. Thürmer, Phys. Rev. Lett. **102** (2009) 136101.

[9] M. Zinke-Allmang, L. C. Feldman, and M. H. Grabow, Surf. Sci. Rep. **16** (1992) 377.

[10] D. A. Huse, Phys. Rev. B **34** (1986) 7845.

[11] H.-J. Ernst, F. Fabre, and J. Lapujoulade, Phys. Rev. Lett. **69** (1992) 458.

[12] R. Schuster, D. Thron, M. Binetti, X. Xia, and G. Ertl, Phys. Rev. Lett. **91** (2003) 066101.

[13] W. W. Pai, J. F. Wendelken, C. R. Stoldt, P. A. Thiel, J. W. Evans, and D. Liu, Phys. Rev. Lett. **86** (2001) 3088.

[14] J. D. Erlebacher and M. J. Aziz, Surf. Sci. **374** (1997) 427.

[15] T. Irisawa, Y. Arima, J. Cryst. Growth **163** (1996) 22.

[16] The time unit Δt for a trial of the movement is so chosen that the diffusion coefficient of an isolated adatom is $e^{-E_{\rm d}/k_{\rm B}T}/4$, where $E_{\rm d}$ is the diffusion barrier for an isolated adatom.

[17] This could be a reason for the discrepancy in the time scales of the experiment and the simulation.